Dominant *ARL3*-related Retinitis Pigmentosa

Josephine Prener Holtan[1,2], Knut Teigen[3], Ingvild Aukrust[4], Ragnheiður Bragadóttir [1,2], Gunnar Houge[4]

[1]Department of Ophthalmology, Oslo University Hospital, Oslo, Norway

[2]Institute of Clinical Medicine,University of Oslo, Oslo, Norway

[3]Department of Biomedicine, University of Bergen, Bergen, Norway

[4]Department of Medical Genetics, Haukeland University Hospital, Bergen, Norway

Correspondence to:

Josephine Prener Holtan

Department of Ophthalmology

Oslo University Hospital,

Postboks 4956, Nydalen,

N-0424 Oslo, Norway.

Tel: +4722118589 / Fax: +4722119989

Email: josephih@uio.no

jospre@ous-hf.no,

words abstract: 248

words article: 1890

Tables: 0

Figures: 4

ABSTRACT

PURPOSE: To clinically and genetically characterise a second family with dominant *ARL3*-related retinitis pigmentosa due to a specific *ARL3* missense variant, p.(Tyr90Cys).

METHODS: Clinical examination included optical coherence tomography, electroretinography, and ultra-wide field retinal imaging with autofluorescence. Retrospective data were collected from the registry of inherited retinal diseases at Oslo university hospital. DNA was analysed by whole-exome sequencing and Sanger sequencing. The *ARL3* missense variant was visualized in a 3D-protein structure.

RESULTS: The phenotype was non-syndromic retinitis pigmentosa with cataract associated with early onset of decreased central vision and central retinal thinning. Sanger sequencing confirmed the presence of a de novo *ARL3* missense variant p.(Tyr90Cys) in the index patient and his affected son. We did not find any other cases with rare *ARL3* variants in a cohort of 431 patients with retinitis pigmentosa-like disease. By visualizing Tyr90 in the 3D protein structure, it seems to play an important role in packing of the α/β structure of ADP-ribosylation factor-like 3 (ARL3). When changing Tyr90 to cysteine, we observe a loss of interactions in the core of the α/β structure that is likely to affect folding and stability of ARL3.

CONCLUSION: Our study confirms that the *ARL3* missense variant p.(Tyr90Cys) causes retinitis pigmentosa. In 2016, Strom et al. reported the exact same variant in a mother and two children with RP, labelled ?RP83 in the OMIM database. Now the questionmark can be removed, and *ARL3* should be added to the list of genes that may cause non-syndromic dominant retinitis pigmentosa.

Keywords: *ARL3*, autofluorescence, retinitis pigmentosa, retinal dystrophy

INTRODUCTION

Retinitis pigmentosa (RP) is a highly heterogeneous genetic disease with progressive degeneration of the light-sensitive photoreceptors. The disease primarily affects the rods, but through apoptosis-like mechanism the cones can be secondarily affected, termed rod-cone dystrophy. The photoreceptor degeneration causes nyctalopia, narrowing of the visual field and in some cases loss of central vision. RP can be part of a syndrome, e.g. ciliopathies affecting multiple organ systems, but the most common is non-syndromic RP (1). Non-syndromic RP can have recessive, dominant and X-linked inheritance, and 71 causative genes are so far known (www.retnet.org). Most of these genes code for proteins involved in the visual cycle and photoreceptor function. The great clinical variability of RP is a consequence of this genetic heterogeneity and variable expressivity of different pathogenic genetic variants (mutations). This is reflected by differences in age of symptom debut, progression rate and pattern of retinal degeneration. Sometimes the same gene can cause dominant and recessive forms of rod-cone dystrophy, where the dominant form is usually milder (2). One example is *PRPH2* related disease [MIM:179605], where dominant mutations are associated with late onset RP with limited central vision loss, while the recessive form usually causes severe rod-cone dystrophy, with early onset of symptoms and loss of vision in the first decade of life (3, 4).

There are many patients with RP of unknown genetic cause (5). Several new candidate genes have recently been found. One of these is ADP-ribosylation factor-like 3; *ARL3* [MIM: 604695], encoding a ras-like GTP-binding protein belonging to the ARF family. Its activity is regulated by ARL13b (a GTP-exchange factor; a GEF) and RP2 (a GTPase activating protein; a GAP). GTP-bound ARL3 facilitates transport of cargo complexes through the interconnecting

cilium of the photoreceptors, and these contain e.g. outer segment proteins (rhodopsin kinase, transducin) and lipid-binding proteins (UNC1119, PDEδ). Upon RP2-stimulated GTP hydrolysis, cargo is released in the outer segment (6-9).

The missense *ARL3* variant (NM_004311.3) c.269A>G, p.(Tyr90Cys), has previously been reported as a possible cause of non-syndromic autosomal dominant RP in a mother and her two children (10). In addition, homozygocity for two different *ARL3* Arg149 missense variants were recently reported to cause Joubert syndrome (11). Possibly, alterations in *ARL3* may cause a spectrum of phenotypes, depending on the biochemical consequence of the mutation and inheritance pattern. The aim of this study was therefore to clinically and genetically characterise a family with RP harboring a missense variant in *ARL3* (c.269A>G, p.Tyr90Cys), including a retrospective four-year follow-up of the index patient.

MATERIALS AND METHODS

Patient Samples

All four individuals in the study (father, son and both parents of the father) provided signed informed consent that their clinical and genetic data could be used for research purposes. Retrospective data was collected from the registry of inherited retinal diseases, Oslo University hospital and from medical records. Biological material was collected from the biobank of inherited retinal diseases, Oslo University Hospital. The study was conducted after approval from the Regional Ethics Committee, South East Norway, REK #2015/2166.

Phenotype description

The phenotype description included electroretinography (ERG), Goldman perimetry (father only), ultra-wide field retinal images (UWF) with red-green and fundus autofluorescence (532nm) images (Optos 200tx and Optos California), and optical coherence tomography (OCT). ERG was performed using standard ISCEV procedure (12).

Genetic testing

Rare variants were identified using next-generation sequencing of 268 genes associated with inherited retinal disease. Genomic DNA was isolated from blood, and DNA samples were further prepared using the SeqCap EZ MedExome Kit (Roche, Bazel, Switzerland), followed by paired-end 150 nt sequencing on the Illumina NextSeq500. Alignment and variant calling was performed as previously described (13). Average median coverage of the target region was 46X with 100% of *ARL3* covered with at least 20 reads. Data annotation and interpretation were performed using the Cartagenia Bench Lab, NGS module (Cartagenia, Leuven, Belgium). The *ARL3* (NM_004311.3) c.269A>G p.(Tyr90Cys) missense variant found by this approach was later Sanger sequenced for confirmation and family follow-up. The variant was not present in the GnomAD population database and the involved amino acid is well conserved between species. The variant was predicted pathogenic/deleterious by four different *in silico* softwares (Align GVGD, SIFT, MutationTaster and PolyPhen-2).

RESULTS

Patients' phenotypes

Retinitis pigmentosa was diagnosed in a father and his son. The former was 57-years old otherwise healthy man born by non-consanguineous Norwegian parents without any family history of eye disease. He was operated for strabismus (alternating esotropia) at age 6, with persistent stereopsis failure. At age 6 the fundus was described to have a poorly defined optic disc, attenuated retinal arteries and pigment changes in the inferior part of the retina. The patient retrospectively reported nyctalopia from age 6, narrowing of the visual field from early adulthood, and reduced central vision from his thirties. The diagnosis of RP was verified by ERG at age 39 and ERG was repeated at age 53. Both ERGs showed extinguished scotopic and photopic response. Visual acuity at age 38 was 0.25 (20/80) in both eyes. Fourteen years later, the visual acuity was around 0.16 to 0.1 (20/125 to 20/200) and remained stable from age 52 to 57. Intraocular pressures (IOP) was normal. Cataract surgery for bilateral sub-capsular cataract was performed at ages 46 and 55.
Examination at age 57 revealed mild asteroid hyalosis on the right eye and bilateral severe degeneration of the peripheral and posterior poles of the retina (Figure 1). There was concentric narrowing of the visual field with 10 degrees of central vision remaining. OCT revealed central atrophy with no cystic macula changes and central retinal thickness of 120-130 µm in both eyes. UWF with autofluorescence were obtained at age 53 and age 57 (Figure 1).

The son of the index patient was 17-years old. His mother was from Asia and had normal vision and no family history of eye disease. The patient was diagnosed with Tourette's syndrome as a child, treated with aripripaxol 5mg daily. At age 16, an optician discovered

pigment changes in the retina. When questioned he described some difficulty navigating in the dark but denied changes in peripheral vision. Visual acuity on the right eye was 0.63 (20/32) and on the left eye 0.4 to 0.63 (20/50 to 20/32). IOP was normal in both eyes. ERG showed extinguished scotopic response with reduced photopic amplitudes and increased implicit time. OCT demonstrated a central atrophy with no edema and a central retinal thickness of 150 µm. The patient declined having a perimetric examination performed. Examination at age 17 revealed a clear lens, no degeneration of the vitreous and moderate degeneration of the fundus with bone-spicule pigmentation (Figure 2).

Genetic testing

Exome sequencing-based gene panel analysis of 268 genes associated with inherited retinal diseases revealed a heterozygote *ARL3* missense p.(Tyr90Cys) variant in both father and son. The variant findings were confirmed by Sanger sequencing, and the missense change was proven to be de novo in the father after parental testing. For gene panel content, see genetikkportalen.no and the panel "NGS-retinasykdom" which contains *ARL3*. We did not find rare *ARL3* variants in 431 other patients with eye disease (mostly RP) tested with the same gene panel, suggesting that *ARL3* pathogenic variants is a rare cause of RP.

Molecular modelling

The structure of *ARL3* in the GTP-bound form has previously been solved in complex with RP2 by x-ray crystallography (14). We retrieved 3D coordinates of this complex from the protein data bank (accession code 3BH6) and visualized ARL3 in complex with the GTP analog from the crystal structure (see Figure 4A). We observed that Tyr90 sits in a β-sheet of ARL3 and makes interactions with the neighboring sheets, as well as tight interactions with

the central α-helix of ARL3, involving Leu107 and Thr103 (Figure 4B). Thus, Tyr90 seems to have a central role in packing of the α/β structure of *ARL3*. The tight packing of residues in this domain has been shown to be essential for correct folding of G proteins (15, 16). In particular, the folding pathway of the B1 domain of the single domain IgG-binding protein G (GB1) has been extensively studied, and residues in the core of the α/β structure have been pinpointed as essential for the folding mechanism of GB1 (16). Upon mutating Tyr90 to cysteine, we observe a loss of interactions in the core of the α/β structure in ARL3 (Figure 4C) and we speculate that the loss of these interactions might impair correct folding as well as the stability of ARL3.

DISCUSSION

Our patients have dominant non-syndromic type of RP with debut of nyctalopia in the first decade of life, decreased central vision in the second decade of life, and possibly slowing of retinal degeneration in the third decade of life. The retinal dystrophy is associated with cataract, found in our index patient but so far not in his son. Retinal findings were thinning of the central retina with degeneration of the mid-peripheral fundus (Figures 1 and 2). Remarkably, the de novo *ARL3* variant p.(Tyr90Cys) found in this study in both patients was exactly the same as the variant previously described de novo in a mother with RP and inherited by her two affected children (10). They also found a classic pattern of RP and associated cataract, but the two youngest patients both had macula edema, which was not present in our patients.

Well-regulated transport of proteins from the endoplasmatic reticulum through the connecting cilium to the outer segment of the photoreceptors is crucial for visual function.

Unsurprisingly, pathogenic variants in genes facilitating transport through this cilium are associated with various types of retinal dystrophy like Joubert syndrome-associated, X-linked RP and dominant cone-rod dystrophy (9, 17, 18). ARL3-GTP functions as a cargo displacement factor and plays an important role in the delivery of proteins to the outer segments. The rod-*ARL3* $^{-/-}$ knockout mouse model demonstrates an accumulation of lipidated proteins in the inner segments, correlated to dysregulation of ciliogenesis and intraflagellar transport (9) and rapid degeneration of the photoreceptors. The p.(Tyr90Cys) variant is localized in the GTP binding domain and predicted to compromise GTP binding or exchange. From 3D-protein modelling it appears likely that the exchange of tyrosine to cysteine in a β-sheet of ARL3 disrupts interaction with the highly conserved residues Tyr103 and Leu107 in the central α-helix of ARL3, and thus affect the packing of the α/β-structure - a structure that has been shown to be essential for correct folding of G-proteins (16). A loss-of-function mechanism is thus most likely, but if this is combined with a dominant-negative effect due to lack of G-protein exchange from bound cargo, remains unknown.
Homozygocity for two different missense variants to the same position in *ARL3* (Arg149) has recently been reported to cause Joubert syndrome (11). In this article it was discussed whether the patients described by Strom et al. may harbor a second recessive variant in the *ARL3* gene. Given this second report of the same *ARL3* de novo p.(Tyr90Cys) missense variant segregating with dominant and classic non-syndromic RP correlated with cataract, a recessive model of inheritance is highly unlikely. Rather, *ARL3* is another example of a gene with both recessive and dominant modes of inheritance of missense mutations, the former causing severe syndromic disease while the latter causing milder dominant RP.

However, *ARL3* is not a common cause of dominant RP. After whole gene sequencing by gene panel testing, we only found *ARL3* pathogenic variants in 2 of 431 patients with inherited retinal disease.

ACKNOWLEDGEMENTS

Financial support was provided by the Norwegian Association of the Blind and Partially Sighted and Jon S Larsen foundation.

Declaration of interest statement

The authors report no conflict of interest.

FIGURE LEGENDS

Figure 1

Father, age 57 (right eye) (Optomap California). **A:** Composite red-green digital image shows retinal pigment epithelial atrophy and bone-spicule pigmentation mainly present in the mid-periphery, an atrophic optic disc and attenuated vessels. **B:** 532 nm wavelength autofluorescence reveals a widespread hypofluorescent scattered areas in the far-peripheral and mid-peripheral fundus. In the posterior pole, a hyperfluorescence area is present that corresponds to the remaining visual field. In the fovea, hypofluorescence is detected corresponding to the central atrophy on OCT and the patient's reduced central vision. **C**: age 53 (left eye) (Optos 200tx) and **D**: age 57 (left eye) (Optos California): A double hyperfluorescent ring is surrounding the fovea, including central hypofluorescent changes. Four-year follow-up show a minimal change of autofluorescence in the macula.

Figure 2

Son, age 17 (Optos California). **A** (right eye): Composite red-green digital image shows attenuation of the retinal vessels, bone-spicule pigmentation mainly in the superior and inferior retina and ring formed discoloration in the mid periphery. Optic disc is normal. **B** (right eye): Autofluorescent image obtained with 532 nm wavelength reveals hypofluorescent changes in the midperiphery with normal autofluorescence in the nasal section and surrounding macula. **C** (left eye): Detailed autofluorescence of the posterior pole shows an oval hyperfluorescent demarcation around fovea with discrete small hypofluorescent spots.

Figure 3

Family pedigree. *De novo* occurrence of heterozygote *ARL3* p.(Tyr90Cys) variant in index patient with dominant transmission to son.

Figure 4

Structure of ARL3, showing Tyr90 situated in the core of the α/β-structure, close to the GTP binding site (**A**). The side chain of Tyr90 makes interactions with a central α-helix of ARL3, ensuring its tight packing with the β-sheet (**B**). When Tyr90 is mutated to a cysteine, these interactions are no longer maintained **(C**).

REFERENCES

1. Hartong DT, Berson EL, Dryja TP. Retinitis pigmentosa. Lancet. 2006;368(9549):1795-809.
2. Grondahl J. Estimation of prognosis and prevalence of retinitis pigmentosa and Usher syndrome in Norway. Clin Genet. 1987;31(4):255-64.
3. Farrar GJ, Jordan SA, Kenna P, Humphries MM, Kumar-Singh R, McWilliam P, et al. Autosomal dominant retinitis pigmentosa: localization of a disease gene (RP6) to the short arm of chromosome 6. Genomics. 1991;11(4):870-4.
4. Wang F, Wang H, Tuan HF, Nguyen DH, Sun V, Keser V, et al. Next generation sequencing-based molecular diagnosis of retinitis pigmentosa: identification of a novel genotype-phenotype correlation and clinical refinements. Hum Genet. 2014;133(3):331-45.
5. Carss KJ, Arno G, Erwood M, Stephens J, Sanchis-Juan A, Hull S, et al. Comprehensive Rare Variant Analysis via Whole-Genome Sequencing to Determine the Molecular Pathology of Inherited Retinal Disease. Am J Hum Genet. 2017;100(1):75-90.
6. Cavenagh MM, Breiner M, Schurmann A, Rosenwald AG, Terui T, Zhang C, et al. ADP-ribosylation factor (ARF)-like 3, a new member of the ARF family of GTP-binding proteins cloned from human and rat tissues. J Biol Chem. 1994;269(29):18937-42.
7. Ismail SA, Chen YX, Rusinova A, Chandra A, Bierbaum M, Gremer L, et al. Arl2-GTP and Arl3-GTP regulate a GDI-like transport system for farnesylated cargo. Nat Chem Biol. 2011;7(12):942-9.
8. Kuhnel K, Veltel S, Schlichting I, Wittinghofer A. Crystal structure of the human retinitis pigmentosa 2 protein and its interaction with Arl3. Structure. 2006;14(2):367-78.
9. Hanke-Gogokhia C, Frederick JM, Zhang H, Baehr W. Binary Function of ARL3-GTP Revealed by Gene Knockouts. Adv Exp Med Biol. 2018;1074:317-25.
10. Strom SP, Clark MJ, Martinez A, Garcia S, Abelazeem AA, Matynia A, et al. De Novo Occurrence of a Variant in ARL3 and Apparent Autosomal Dominant Transmission of Retinitis Pigmentosa. PLoS One. 2016;11(3):e0150944.

11. Alkanderi S, Molinari E, Shaheen R, Elmaghloob Y, Stephen LA, Sammut V, et al. ARL3 Mutations Cause Joubert Syndrome by Disrupting Ciliary Protein Composition. Am J Hum Genet. 2018;103(4):612-20.
12. McCulloch DL, Marmor MF, Brigell MG, Hamilton R, Holder GE, Tzekov R, et al. ISCEV Standard for full-field clinical electroretinography (2015 update). Doc Ophthalmol. 2015;130(1):1-12.
13. Bredrup C, Johansson S, Bindoff LA, Sztromwasser P, Krakenes J, Mellgren AE, et al. High myopia-excavated optic disc anomaly associated with a frameshift mutation in the MYC-binding protein 2 gene (MYCBP2). Am J Ophthalmol. 2015;159(5):973-9.e2.
14. Veltel S, Gasper R, Eisenacher E, Wittinghofer A. The retinitis pigmentosa 2 gene product is a GTPase-activating protein for Arf-like 3. Nat Struct Mol Biol. 2008;15(4):373-80.
15. Lapidus LJ, Acharya S, Schwantes CR, Wu L, Shukla D, King M, et al. Complex pathways in folding of protein G explored by simulation and experiment. Biophys J. 2014;107(4):947-55.
16. Kmiecik S, Kolinski A. Folding pathway of the b1 domain of protein G explored by multiscale modeling. Biophys J. 2008;94(3):726-36.
17. Graham TR. Membrane targeting: getting Arl to the Golgi. Curr Biol. 2004;14(12):R483-5.
18. Grayson C, Bartolini F, Chapple JP, Willison KR, Bhamidipati A, Lewis SA, et al. Localization in the human retina of the X-linked retinitis pigmentosa protein RP2, its homologue cofactor C and the RP2 interacting protein Arl3. Hum Mol Genet. 2002;11(24):3065-74.

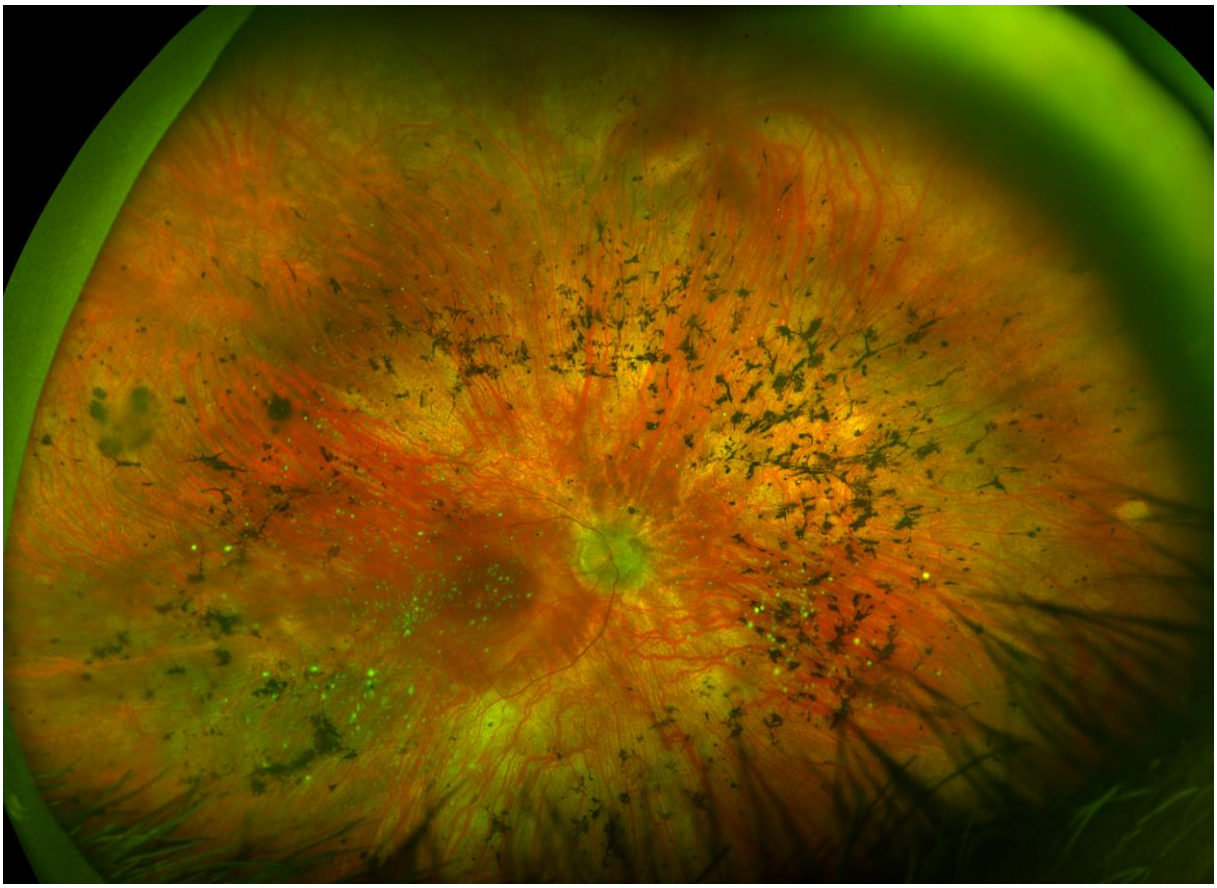

Figure 1A

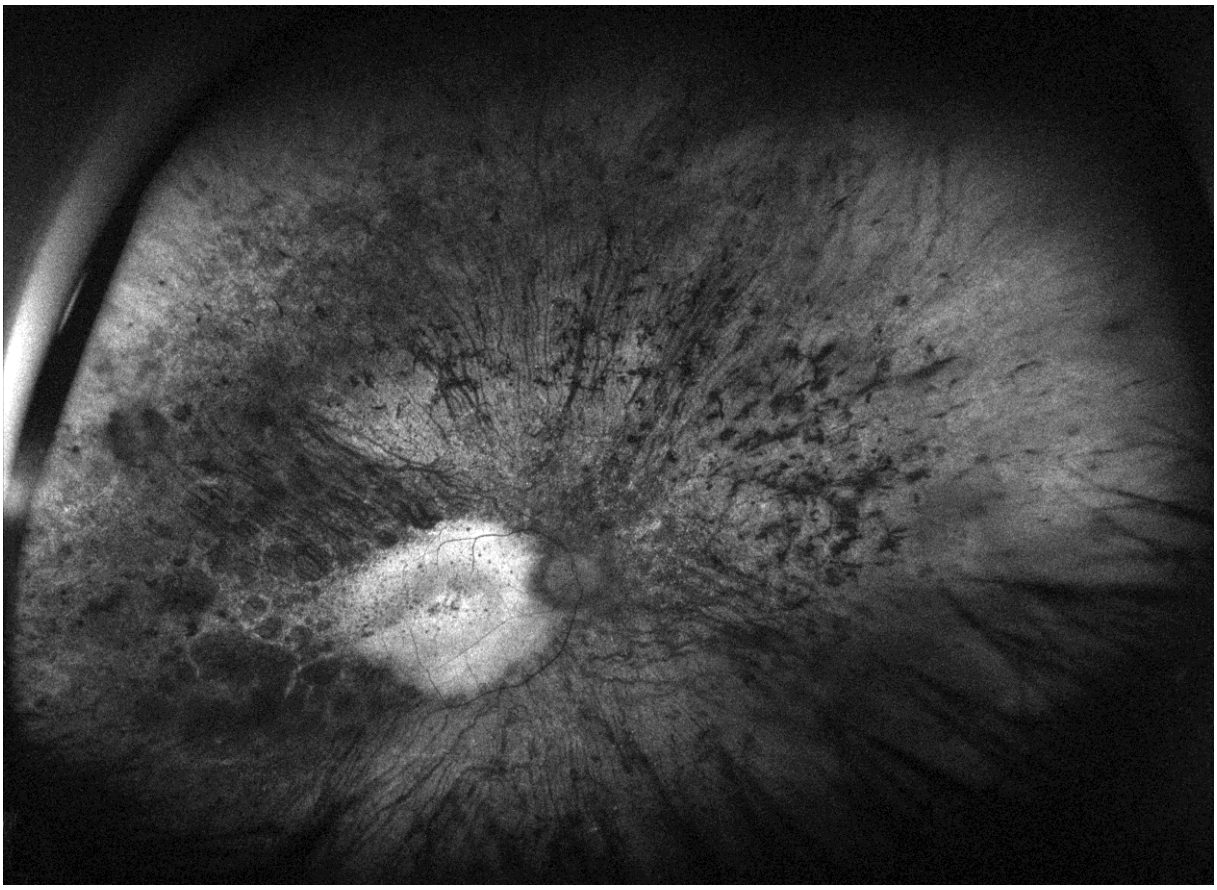

Figure 1B

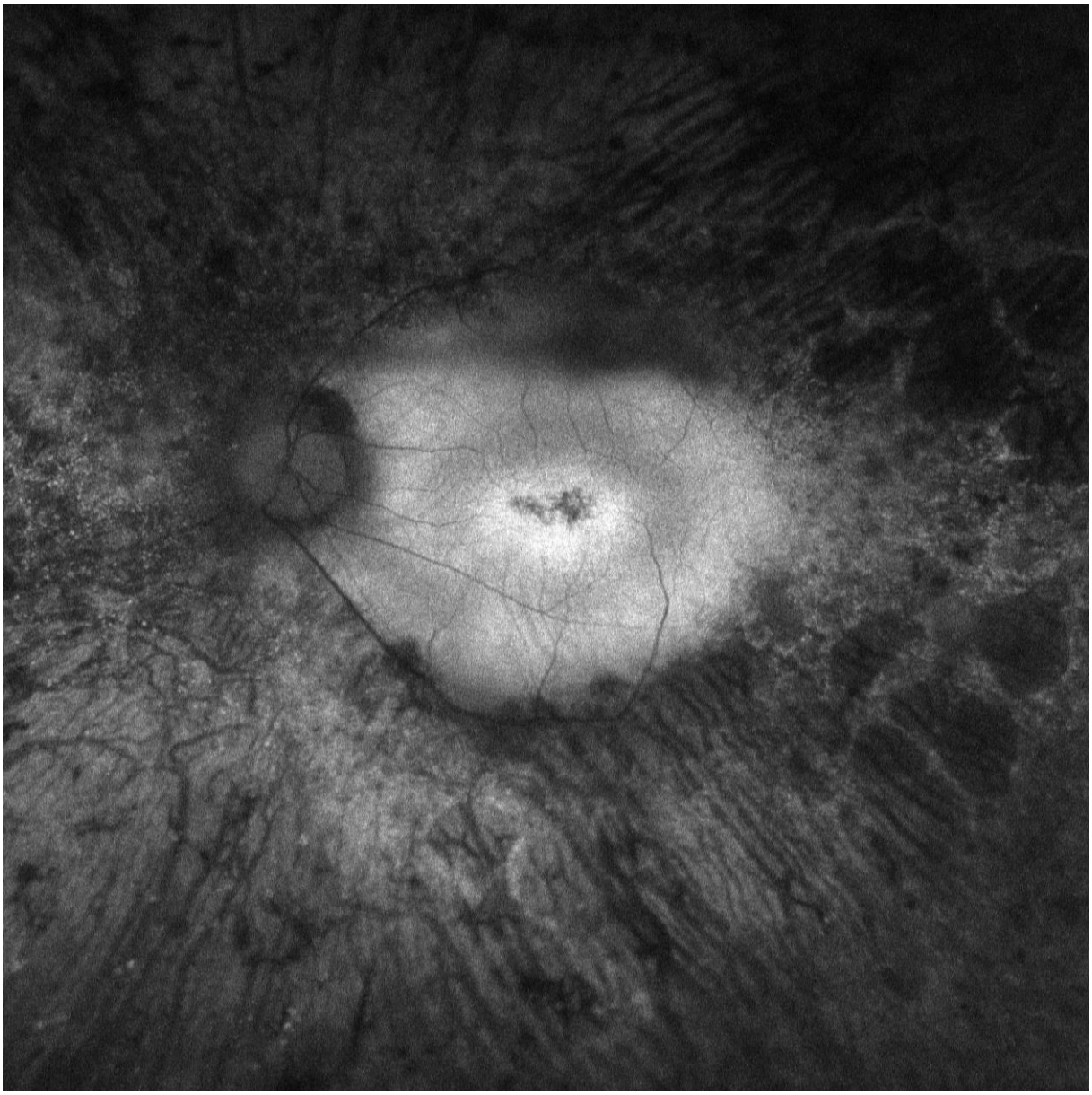

Figure 1C

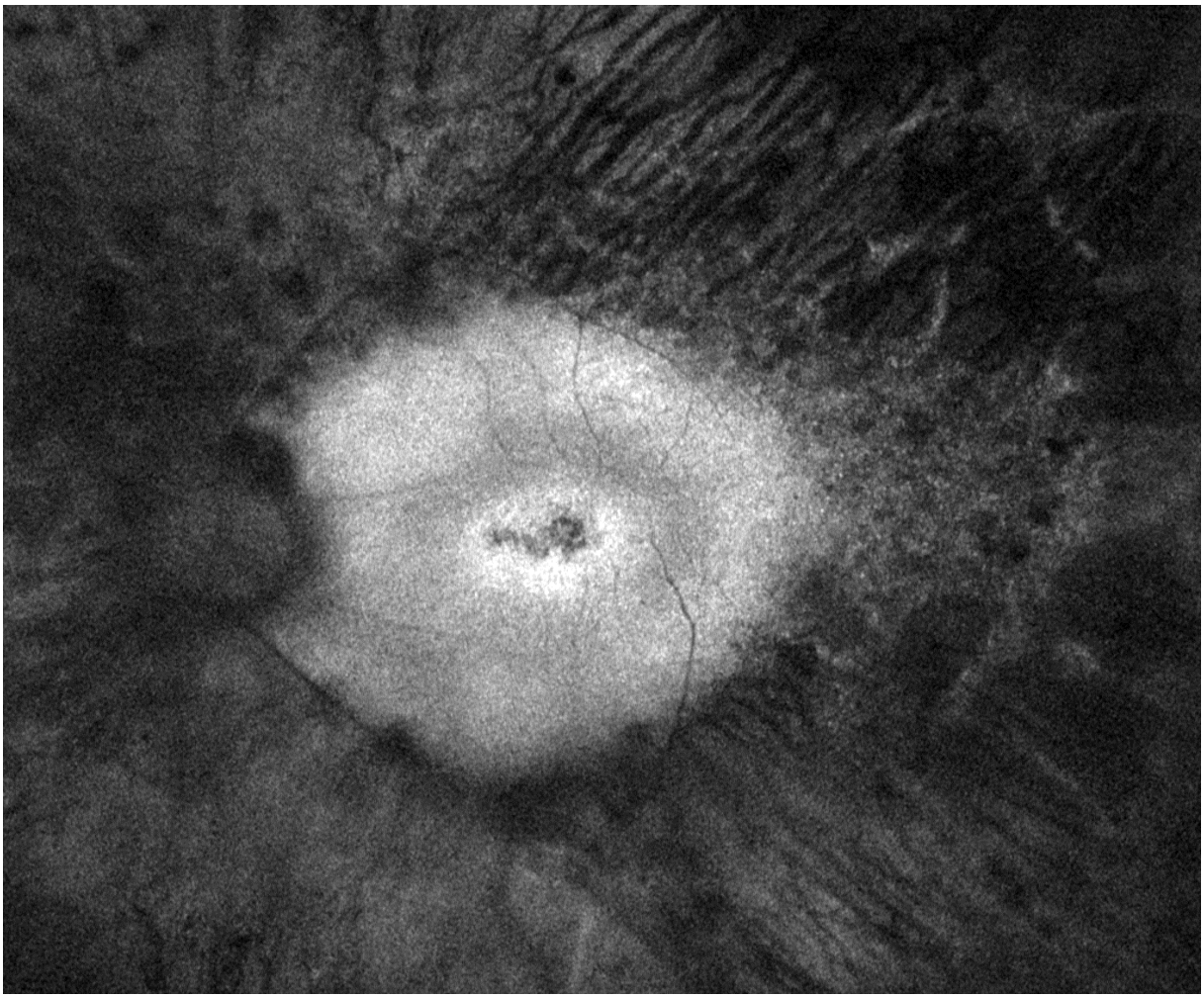

Figure 1D

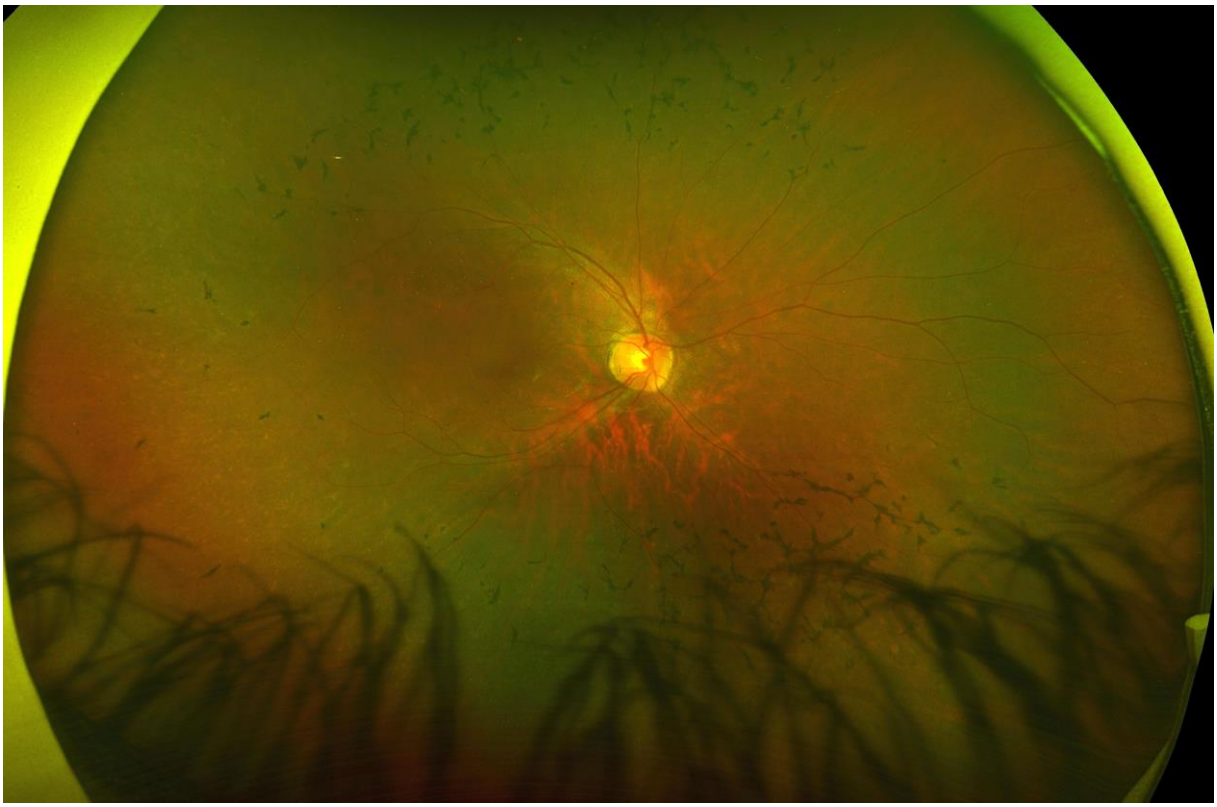

Figure 2A

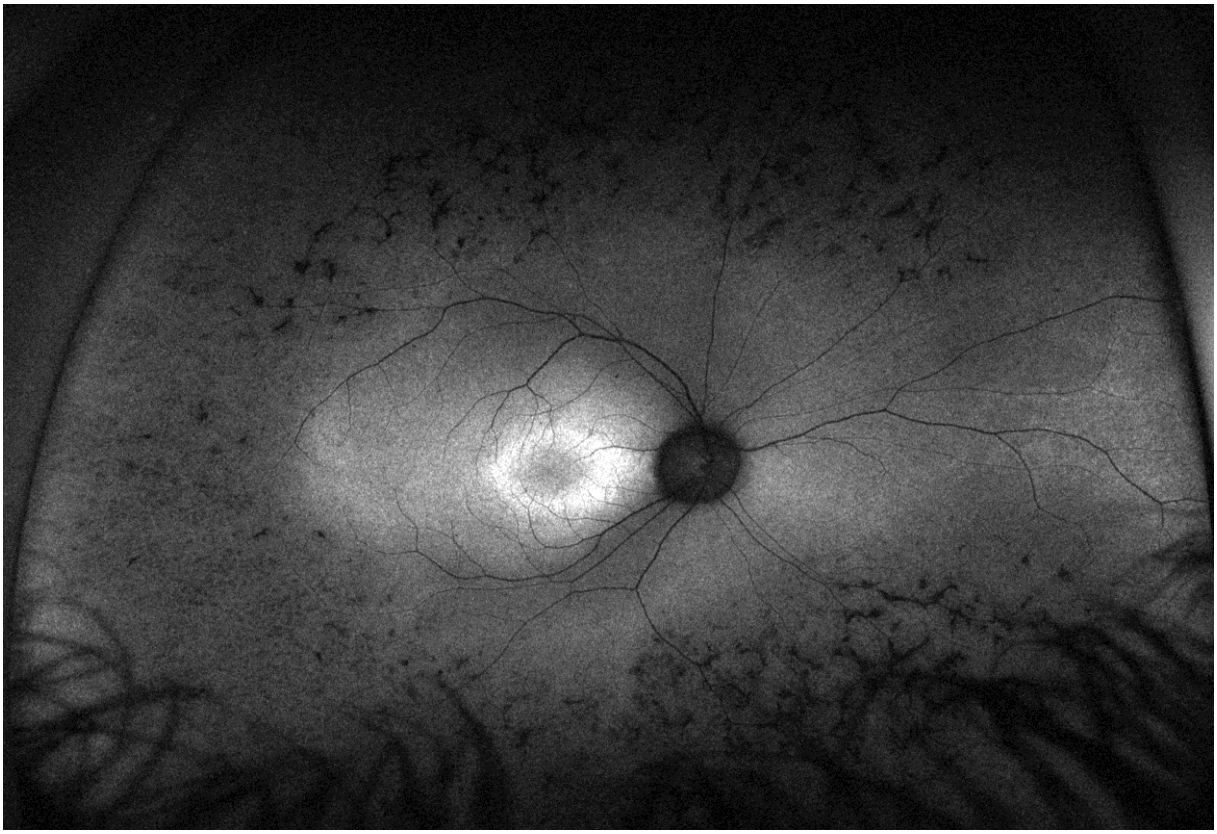

Figure 2B

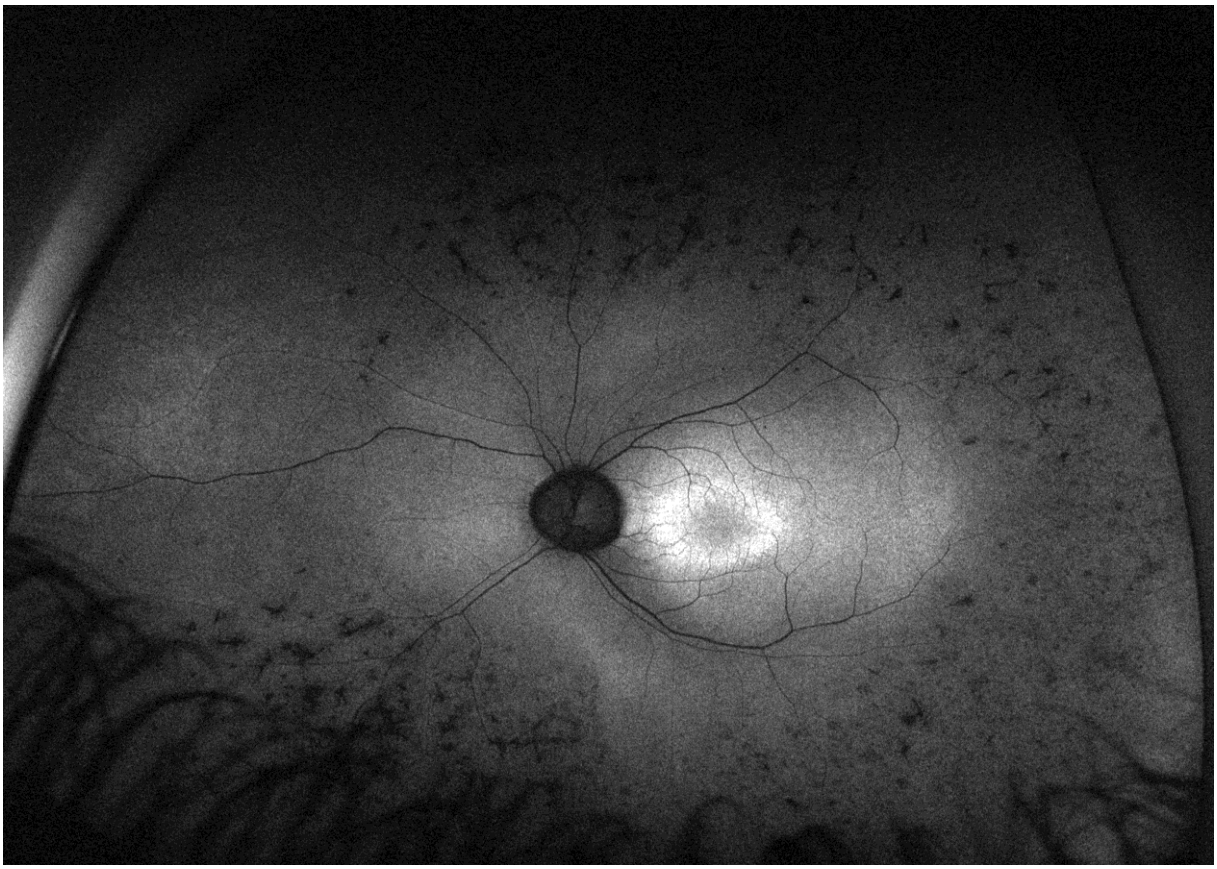

Figure 2C

Figure 3

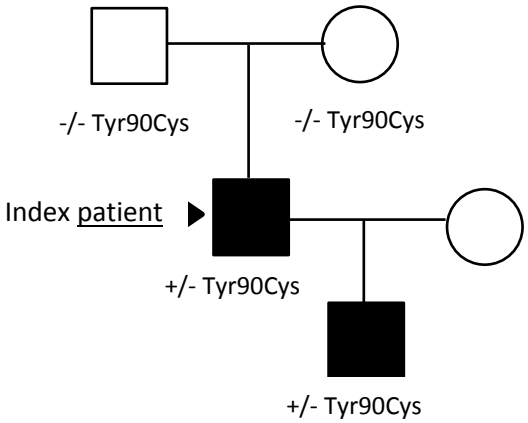

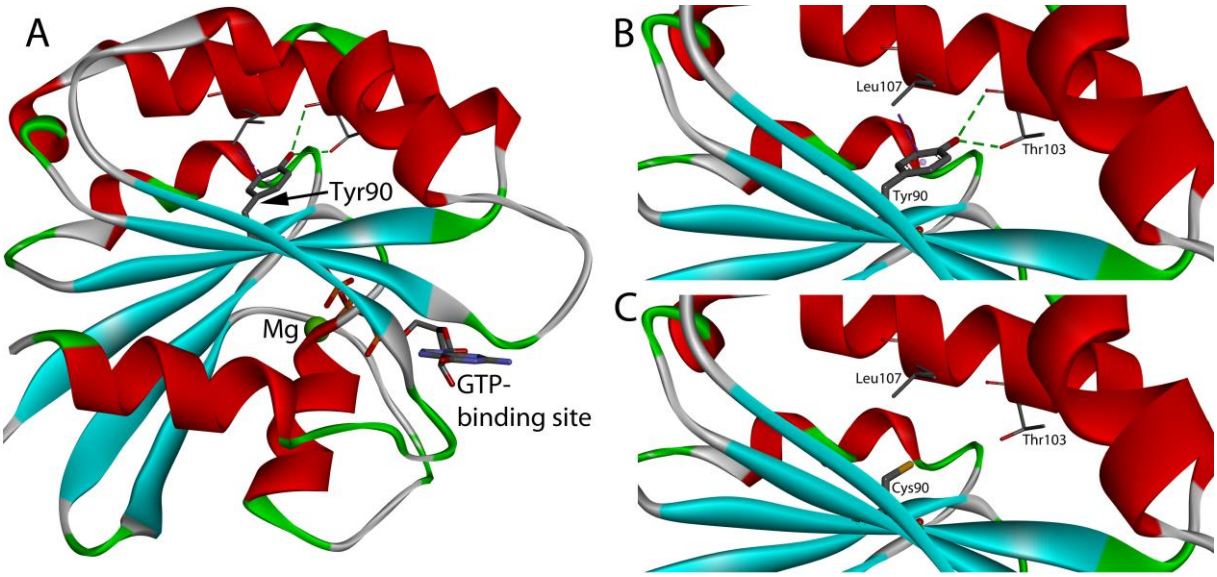

Figure 4

Figure Captions

Figure 1: Father, age 57 (right eye) (Optomap California)(**A,B**). **A:** Composite red-green digital image shows pigment epithelial atrophy and bone-spicule pigmentation mainly present in the mid-periphery, an atrophic optic disc and attenuated vessels. **B:** 532 nm wavelength autofluorescence reveals widespread hypofluorescent scattered areas in the far-peripheral and mid-peripheral fundus. In the posterior pole, a hyperfluorescencent area is present that corresponds to the remaining visual field. In the fovea, hypofluorescence is detected corresponding to the central atrophy on OCT and the patient's reduced central vision. **C**: age 53 (left eye) (Optos 200tx) and **D**: age 57 (left eye) (Optos California): A double hyperfluorescent ring surrounding the fovea, including central hypofluorescent changes. Four-year follow-up shows a minimal change of autofluorescence in the macula.

Figure 2: Son, age 17 (Optos California). **A** (right eye): Composite red-green digital image shows attenuation of the retinal vessels, bone-spicule pigmentation mainly in the superior and inferior retina and ring formed discoloration in the mid periphery. Optic disc is normal. **B** (right eye): Autofluorescent image obtained with 532 nm wavelength reveals hypofluorescent changes in the midperiphery with normal autofluorescence in the nasal

section and surrounding macula. **C** (left eye): Detailed autofluorescence of the posterior pole shows an oval hyperfluorescent demarcation around fovea with discrete small hypofluorescent spots.

Figure 3: Family pedigree. *De novo* occurrence of heterozygote *ARL3* p.(Tyr90Cys) variant in index patient with dominant transmission to son.

Figure 4: Structure of ARL3, showing Tyr90 situated in the core of the α/β-structure, close to the GTP binding site (**A**). The side chain of Tyr90 makes interactions with a central α -helix of ARL3, ensuring its tight packing with the β-sheet (**B**). When Tyr90 is mutated to a cysteine, these interactions are no longer maintained (**C**).